Available online at www.sciencedirect.com
SCIENCE DIRECT®
Journal of Power Sources 122 (2003) 122–131
JOURNAL OF POWER SOURCES
www.elsevier.com/locate/jpowsour

Study of Ni-samaria-doped ceria anode for direct oxidation of methane in solid oxide fuel cells

Jenshi B. Wang [a], Jiun-Ching Jang [b], Ta-Jen Huang [b,*]

[a] *Department of Chemical Engineering, I-Shou University, Kaohsiung 840, Taiwan, ROC*
[b] *Department of Chemical Engineering, National Tsing Hua University, Hsinchu 300, Taiwan, ROC*

Received 7 January 2003; accepted 3 March 2003

Abstract

A Ni-samaria-doped ceria (SDC) anode is employed for direct electrochemical oxidation of methane in a solid oxide fuel cell (SOFC) with yttria-stabilized zirconia (YSZ) as electrolyte to seek insights into the properties and electrocatalytic activity of the anode. Compared with Ni-YSZ, the Ni-SDC anode exhibits higher open-circuit voltages (OCVs) and a lower degree of polarization. The anodic polarization of Ni-SDC is shown to result from the effect of concentration polarization. The effect of nickel content in Ni-SDC on the performance and microstructure of the anode are studied. It is found that the anodic polarization and electrocatalytic activity strongly depend on the Ni content in the anode, and optimum results are achieved with 60 wt.% Ni. The good performance of this Ni-SDC anode appears to be due to its microstructure. In addition, the anode is stable in a methane environment.

Keywords: Solid oxide fuel cell; Direct methane oxidation; Samaria-doped ceria; Nickel; Open-circuit voltage; Anode microstructure

1. Introduction

Most fuel cells currently in experimental use or under development operate with hydrogen as the fuel. Hydrogen is industrially produced in an economical way by the reforming of hydrocarbons [1]. The use of reformers in fuel cell systems to convert hydrocarbon fuel to hydrogen leads to significant complications and loss of fuel efficiency, which make the wide-spread use of the fuel cell not a practical reality in the near future. Thus, developing fuel cells based on direct oxidation of hydrocarbons, such as methane, appears as a viable alternative and may lead to the near-term commercialization of such devices [2,3].

The catalytic activity of the anode is known to be important in the design of solid oxide fuel cells (SOFCs) that are capable of direct electrocatalytic oxidation of methane and other hydrocarbon fuels. Since conventional nickel-yttria-stabilized zirconia (Ni-YSZ) anodes have several drawbacks, research efforts have been undertaken to develop new anodic electrocatalysts. Ceria has long been used as an effective component in three-way catalysts for automotive exhaust control [4,5]. The ability of ceria to achieve stable operation in a methane environment on catalysts [6] and on electrodes [7–9] has been reported. Thus, in the search of high-performance SOFC anodes, ceria and doped ceria have been evaluated as possible anode materials [2,9–12]. Murray et al. [2] employed an anode of composite Ni-YSZ and yttria-doped ceria layers for dry methane fuels to attain a power density comparable with that of hydrogen fuel cells and still maintain stable operation between 500 and 700 °C. Gorte et al. [9] concluded that although a Cu-YSZ cermet anode was stable during hydrocarbon oxidation, reasonable power densities could only be achieved with addition of ceria. Rare earth-doped ceria is known to exhibit mixed ionic and electronic conductivity under reducing atmospheres [13,14]. Samaria is one of the best possible dopants to modify the structural and chemical properties of ceria because of the similarity in the ionic radius and the electronegativity [15]. Among the aliovalent cation-doped ceria, samaria-doped ceria (SDC) possesses the highest ionic conductivity [16]. Although the benefits of using SDC as an anode material to lower the operating temperatures of SOFCs for the electrochemical oxidation of hydrogen [17–19] have been recognized, there has been a dearth of work concerning the use of SDC as anode material for the direct oxidation of methane.

The aim of this paper is to elucidate the anodic properties of Ni-SDC, as well as to examine further the role that the microstructure of Ni-SDC plays in the anodic properties and electrocatalytic activities. For this goal, different Ni-SDC anodes have been prepared for various nickel contents, on

* Corresponding author. Tel.: +886-3-5716260; fax: +886-3-5715408.
E-mail address: tjhuang@che.nthu.edu.tw (T.-J. Huang).

0378-7753/03/$ – see front matter © 2003 Elsevier Science B.V. All rights reserved.
doi:10.1016/S0378-7753(03)00438-5

which studies of anodic polarization and electrocatalytic activities have been performed.

2. Experimental

2.1. Preparation of SDC, Ni-SDC and Ni-YSZ electrocatalysts

SDC was prepared from reagent-grade (99.999% purity, Strem Chemical) $Sm(NO_3)_3{\cdot}6H_2O$ and $Ce(NO_3)_3{\cdot}6H_2O$ by a co-precipitation method. Appropriate amount of samarium nitrate and cerium nitrate in an atomic molar ratio of Sm:Ce = 2:8 were dissolved in deionized water. Hydrolysis of the metal salts to hydroxides was obtained by slowly dropping the solution into NH_4OH solution with stirring to keep the pH > 9. A deep-purple precipitate/gel was formed. A centrifuge was employed to isolate the gel, which was then washed twice by deionized water and octanol. After washing, the gel was dried under vacuum at 110 °C for 4 h, ground, and then calcined in air at 700 °C for 5 h. Afterwards, the prepared SDC was slowly cooled to room temperature.

The Ni-YSZ and Ni-SDC electrocatalysts were prepared by impregnating YSZ (8 mol% yttria, particle size <3 μm, Tosoh, Japan), and the above-prepared SDC power with appropriate amounts of an aqueous solution of nickel nitrate, $Ni(NO_3)_2{\cdot}3H_2O$ (99.999% purity, Strem) for 7 h to obtain various nickel contents with respect to the weight of YSZ or SDC. After evaporating the excess water at 80 °C, the elctrocatalysts were dried under vacuum at 80 °C for 12 h, and then calcined in air at 700 °C for 5 h. The calcination of SDC and electrocatalysts was conducted by passing air at a rate of 1 l min^{-1}, and by ramping the temperature at a rate of 10 °C min^{-1} from room temperature.

The BET surface areas of the Ni-YSZ and Ni-SDC electrocatalysts were determined by means of nitrogen physisorption with a thermal conductivity detector instrument (Quantachrome, USA).

2.2. Preparation and construction of cell

A YSZ solid tube (8 mol% yttria, Zircoa, USA), closed at one end and 145 mm (length) × 25.4 mm (i.d.) × 3 mm (thickness) in dimensions, was employed to fabricate an anode–electrolyte–cathode assembly, with the base of the tube serving as electrolyte. The anode and cathode compartments were constructed on the inner and outer sides of the tube base, respectively. To prepare the reference and counter electrodes, a layer of Pt paste (C3605P, Heraeus) was painted on to the outer side of the tube base. The tube was then fired in a furnace at 400 °C for 2 h, and then at 1000 °C for another 2 h. The working electrode was prepared by painting a thin layer of electrode paste, made with Ni-SDC powders and an ethylene glycol binder, on to the inner side of the tube base, then firing at 200 °C for 2 h, and at 700 °C for a further 2 h.

The anode compartment was sealed by a water-cooled silicone gasket fixed on the top of the YSZ tube. The anode was then reduced in a flow of hydrogen for 12 h to assure metallic nickel in the Ni-SDC anode. The cell was mounted in an insulated electric furnace which was equipped with a Eurotherm 812 temperature programmable controller to ramp or isothermally control the cell temperature. A K-type thermocouple was inserted close to the anode to measure and control the cell temperature. In order to study the polarization of the anode, a piece of platinum wire was connected, by platinum paste, to the working and reference electrodes, and a high-impedance voltammeter (10 GΩ, HP-34401A) was used to measure the potential of the anode. The electric current supplied at the counter electrode was controlled by a potentiostat–galvanostat.

A gaseous mixture of methane (99.999%, Air Product) and argon (99.9995%, Sanfu) with a composition of CH_4:Ar = 1:9, or methane and oxygen with a composition of CH_4:O_2 = 1:9, as regulated by Hastings HFC-202 mass-flow controllers, was fed to the anode at a total flow rate of 100 ml min^{-1} via a tube through the silicone gasket, while air at the same flow rate was supplied directly to the cathode side. Analysis of the fuel gas before and after the cell was carried out on-line by a gas chromatograph (China Chromatography 9800) equipped with a thermal conductivity detector and a Porapak Q column at 50 °C using argon as a carrier gas to separate CH_4, H_2, CO, and CO_2. Scanning electron micrographs (Jeol JSM-5600) were taken to study the microstructures of Ni-SDC anode with different nickel contents. Temperature-programmed oxidation (TPO) was employed to measure the amount of carbon deposition (coke) on the Ni-SDC anodes after 30 h of operation.

3. Results and discussion

3.1. Anodic properties of Ni-SDC and Ni-YSZ electrocatalysts

As seen from Table 1, the BET areas of the Ni-SDC and Ni-YSZ electrocatalysts decrease with increasing Ni con-

Table 1
BET areas of Ni-SDC and Ni-YSZ anodes with different nickel contents

Anodes	Nickel content (wt.%)	BET area (m^2 g^{-1})
Ni-SDC	0	42.05
	30	41.65
	40	30.62
	50	27.49
	60	29.43
	70	26.14
Ni-YSZ	30	8.43
	40	7.86
	50	6.67
	60	7.43

tent and the areas of Ni-YSZ are much less than those of Ni-SDC. The Ni-SDC exhibits a sudden increase in BET area at a Ni content of 60 wt.%, which corresponds with a well-configured microstructure of the anode, as will be discussed later.

The variation of the open-circuit voltages (OCVs) of Ni-SDC and Ni-YSZ anodes with nickel content for direct oxidation of methane at 600 °C is shown in Fig. 1. The results indicate that the OCVs depend on the Ni content, and the OCV of Ni-SDC is a maximum at 60 wt.% Ni. This suggests that the number of active sites at the three-phase boundary (TPB) increase with increasing Ni content in the electrocatalyst, and that the highest reaction areas at the boundary between Ni, SDC and the fuel gas were obtained with the Ni-SDC anode that contained 60 wt.% nickel. When the Ni loading in Ni-SDC is higher than 60 wt.%, sintering of nickel occurs readily and leads to a decrease of porosity in the anode and a decrease of the reaction areas at the TPB. This lowers the OCV of the anode. In addition, as shown in Fig. 1, the OCVs of Ni-YSZ are smaller than those of Ni-SDC. It appears that fewer active sites exist at the TPB of Ni-YSZ since this has a much smaller BET area than that of Ni-SDC. Furthermore, YSZ is a purely ionic conductor in contrast to the mixed ionic–electronic conductivity exhibited by SDC.

The effect of Ni content on the anodic polarization of Ni-SDC during direct electrochemical oxidation of methane was studies. As a result, plots of the Ni-SDC anode overpotential versus current applied at the counter electrode, which exhibits Tafel-like behavior, are presented in Fig. 2 for various Ni contents in Ni-SDC. Each point of the curve represents a different O^{2-} flux through electrolyte from the cathode to the reaction zone at the TPB of the Ni-SDC anode, and corresponds to a different degree of anodic polarization and electrochemical oxidation rate of methane. Remarkably, the anode containing 60 wt.% Ni, abbreviated as Ni(60)SDC hereafter, gives rise to the highest 'limiting current'. It appears that the highest O^{2-} flux to the active sites at the TPB occurs when the Ni(60)SDC anode was employed. In this regard, the anode overpotential as a function of Ni content in Ni-SDC at a fixed current of 2 mA supplied at the counter electrode is shown in Fig. 3. It is seen that the anodic polarization depends strongly on the Ni content in Ni-SDC, and the Ni(60)SDC anode exhibits the least degree of polarization.

To explore the polarization behavior of Ni-SDC anodes, further, the overpotential of Ni(60)SDC versus current supplied at the counter electrode under methane and in an atmosphere containing methane and oxygen are compared in Fig. 4. It is seen that the anodic polarization of Ni(60)SDC in the methane- and oxygen-containing atmosphere is improved considerably in contrast with that under methane alone. These results demonstrate that the polarization of the Ni-SDC anode is caused primarily by the effect of concentration polarization, due to the relatively slow rate of O^{2-} supply from the cathode. This implies that the reaction rate on the surface of the anode is higher than the O^{2-} supply rate to the active sites at the TPB. Thus, the anode performance is controlled by the rate of O^{2-} supply to the active sites of the anode through the electrolyte.

The overpotential versus current plots of Ni(60)SDC and Ni-YSZ anodes during electrochemical methane oxidation are compared in Fig. 5. It is found that the YSZ-supported anodic electrocatalysts are more seriously polarized than

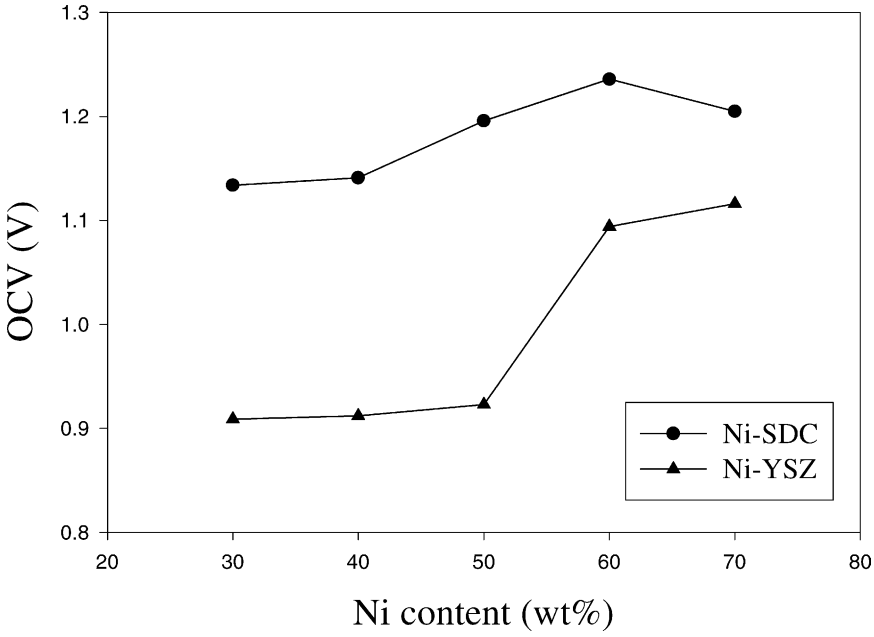

Fig. 1. Variation of open-circuit voltage (OCV) with nickel content for Ni-SDC and Ni-YSZ anodes. Operating conditions: 600 °C; 1 atm; feed composition: CH_4:Ar = 10:90; total flow rate: 100 ml min^{-1}.

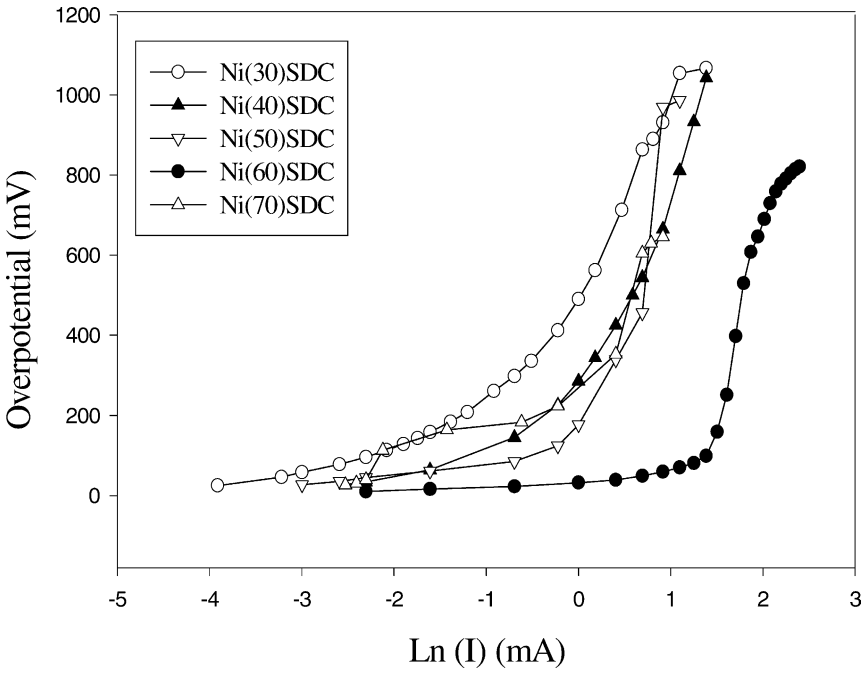

Fig. 2. Plots of overpotential of Ni-SDC anodes vs. current applied at counter electrode for different nickel content in Ni-SDC (operating conditions: same as in Fig. 1).

those supported over SDC. This is ascribed to the fact that the ionic conductivity of SDC is about 30 times that of YSZ at 800 °C [13]. In addition, SDC readily becomes a mixed ionic and electronic conductor in an atmosphere of low oxygen partial pressures [13,14], and is capable of expanding the reaction zone beyond the TPB. As a consequence, the overpotential which results from anodic polarization can be suppressed more effectively by the SDC-supported electrocatalysts. This suggests that SDC is a better support for the anodic electrocatalyst than YSZ.

The long-term stability of Ni(60)SDC as an anodic electrocatalyst has been studied. As depicted in Fig. 6,

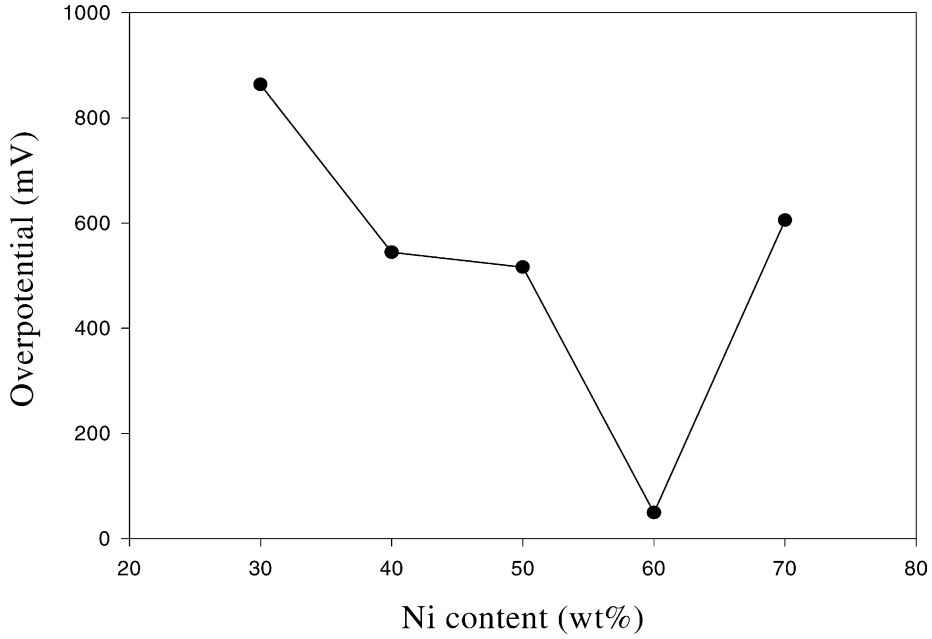

Fig. 3. Anodic overpotential as function of Ni content in Ni-SDC at fixed current of 2 mA supplied at counter electrode (operating conditions: same as in Fig. 1).

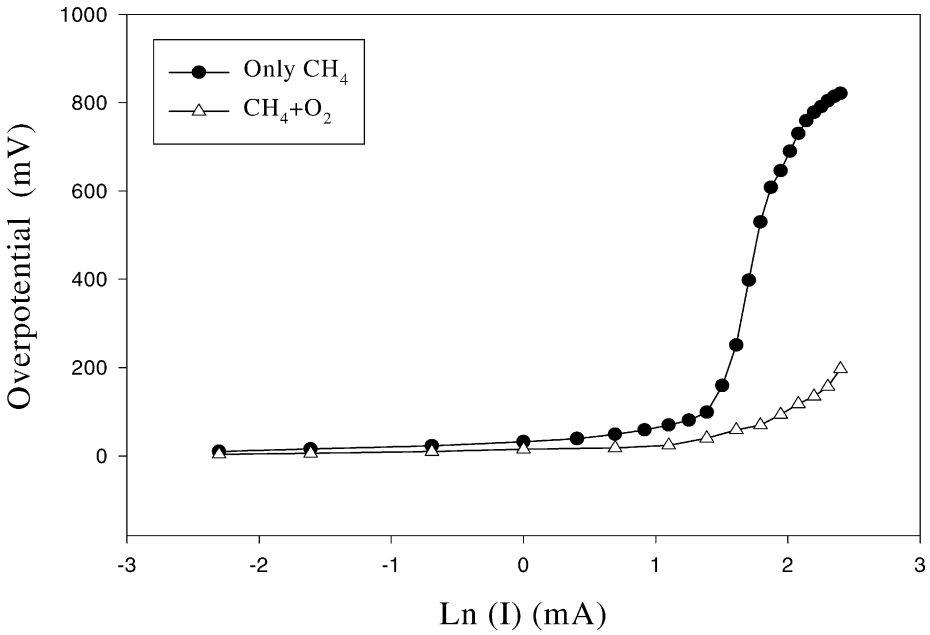

Fig. 4. Plots of overpotential of Ni(60)SDC vs. current supplied at counter electrode under methane (feed composition: CH_4:Ar = 10:90), and in atmosphere of methane and oxygen (feed composition: CH_4:O_2 = 10:90) (operating conditions: 60 °C, 1 atm; total flow rate: 100 ml min^{-1}).

with a fixed current of 4 mA supplied at the counter electrode, the overpotential due to anodic polarization is stabilized at about 101 mV for as long as 30 h. Thus, the structure of Ni(60)SDC can remain stabilized, with negligible deterioration and with the least degree of polarization, for an extended period of time. This is presumably associated with the particular microstructure of the Ni-SDC anode of 60 wt.% Ni content, as will be discussed later.

In summary, compared with other anodic catalysts tested, Ni(60)SDC displays combinations of electrochemical characteristics desirable for an anodic electrocatalyst for direct oxidation of methane; namely: higher OCV, lower polarization overpotential, and enhanced electrode stability.

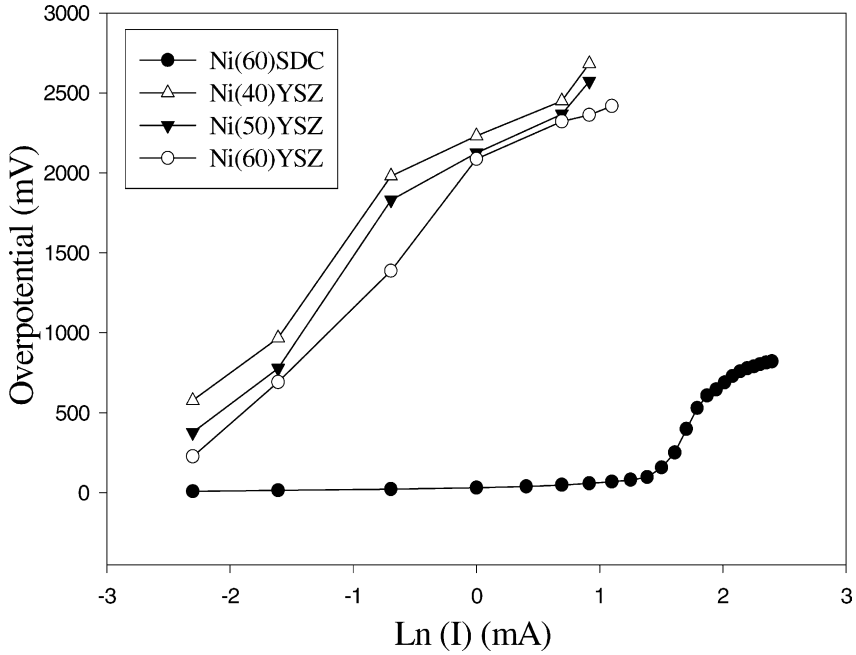

Fig. 5. Comparison of overpotential of Ni(60)SDC and Ni-YSZ anodes of 40–60 wt.% Ni vs. current applied at counter electrode (operating conditions: same as in Fig. 1).

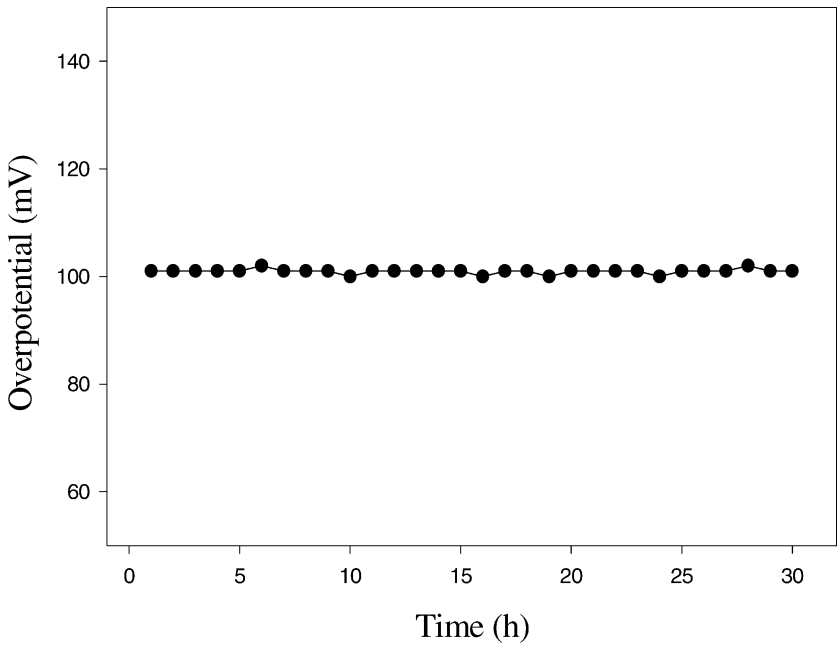

Fig. 6. Overpotential of Ni(60)SDC as function of time, with a fixed current of 4 mA supplied at counter electrode (operating conditions: same as in Fig. 1).

3.2. Electrocatalytic activities and microstructures of Ni-SDC anodes

The time-dependent methane conversion and the specific activities of H_2 and CO formation over Ni(30)SDC and Ni(60)SDC anodes are shown in Figs. 7 and 8, respectively, for direct oxidation of methane under open-circuit operation for 30 h. It is found that, over Ni(60)SDC, the methane conversion is stabilized at ~85%. The activity of H_2 formation also remains steady, despite the fall-off during the initial stage of operation due to coke formation. By contrast, the methane conversion rate over Ni(30)SDC declines progressively with time. These results suggest that Ni(60)SDC has better anodic catalytic activity and stability than Ni(30)SDC for open-circuit direct methane oxidation.

In general, the factors that can sustain the activity and stability of anodic electrocatalysts in fuel cells are: (i) O^{2-} supply rate from the cathode; (ii) release of lattice oxygen anions from the anodic support; (iii) microstructure of the anodic electrocatalyst. Since the electrocatalytic activity tests shown in Figs. 7 and 8 were conducted in an open-circuit manner, no O^{2-} would come from cathode to react with methane. Evidently, the electrochemical oxidation of methane at the anode involves the release of lattice oxygen anions of SDC, which takes place readily in the reducing atmosphere of the anode compartment. Accompanying the release of a lattice oxygen anion, two electrons (e^-_{SDC}) are liberated. If a highly conductive network of nickel-SDC exists in the anode, which is the case with the Ni(60)SDC anode as will be discussed later, the transfer of electrons from SDC to the adjacent metallic phase of nickel can arise directly after the release of lattice oxygen anions since nickel is a relatively better electron conductor than SDC. This markedly reduces the overpotential of the Ni(60)SDC anode. Since the e^-_{SDC} electrons are rapidly transferred to the adjacent Ni phases (e^-_{Ni}) and then leave the anode through the Pt wire connected to the electrode, lattice oxygen anions are released steadily to participate in the electrochemical oxidation of methane, as can be seen by the sustained activities of CO and H_2 formation over the Ni(60)SDC anode (Fig. 8).

The data in Figs. 7 and 8 suggest that the microstructure of Ni-SDC plays an important role in the performance and stability of the anodic electrocatalyst. It appears that the better performance and stability exhibited by the Ni(60)SDC anode is due to optimization of the anode microstructure at this Ni content, in which good distribution and connection between nickel and SDC were obtained. This enables nickel to form a closely-packed Ni skeleton with well-connected SDC grains that are finely distributed over the Ni grain surfaces [18]. Thus, carbonaceous deposits merely grow on the surfaces of the anodic electrocatalyst, with the least possibility of growing within and, hence, damaging the internal structure of the anode. This can be verified by quantifying the amount of coke formed over the Ni(30)SDC and Ni(60)SDC anodes after 30 h of operation. Two layers of coke are formed over the anode. One can be removed with supersonic vibration in a water bath and is called the 'top layer'; the other is very tightly adhered to the anode and can be removed only with force cut-off, and is called the 'bottom layer'. Additional carbonaceous product is also formed, but can be blown away and is thus not counted as coke. The top and bottom layers of coke taken from the Ni(30)SDC and Ni(60)SDC anodes were ground separately

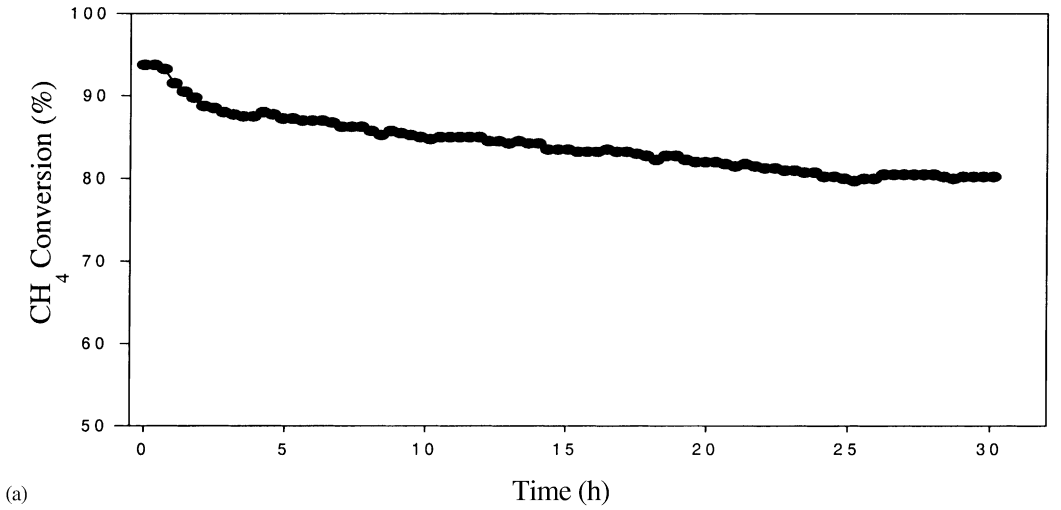

(a)

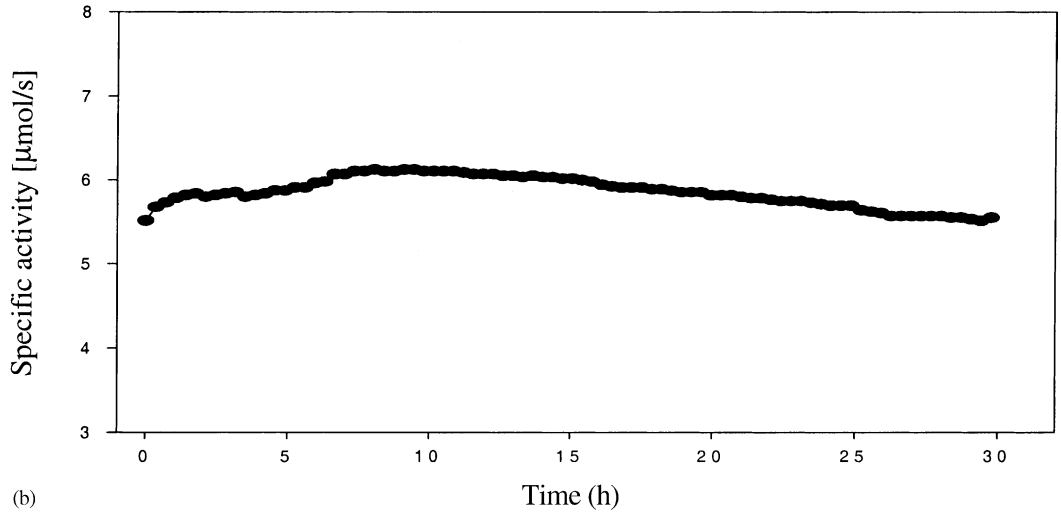

(b)

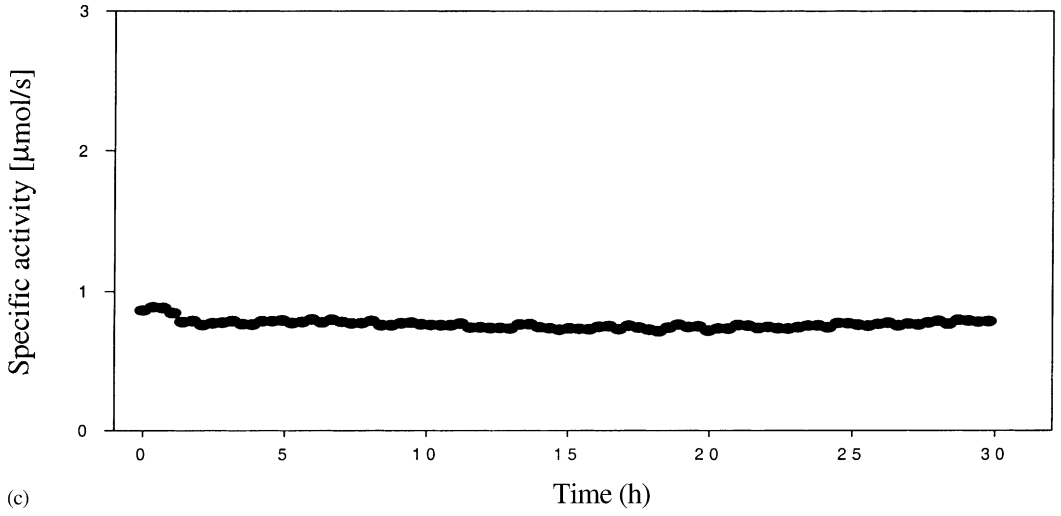

(c)

Fig. 7. (a) Methane conversion, and specific activities of (b) H_2 and (c) CO formation over Ni(30)SDC anode under open-circuit condition as function of time (operating conditions: same as in Fig. 1).

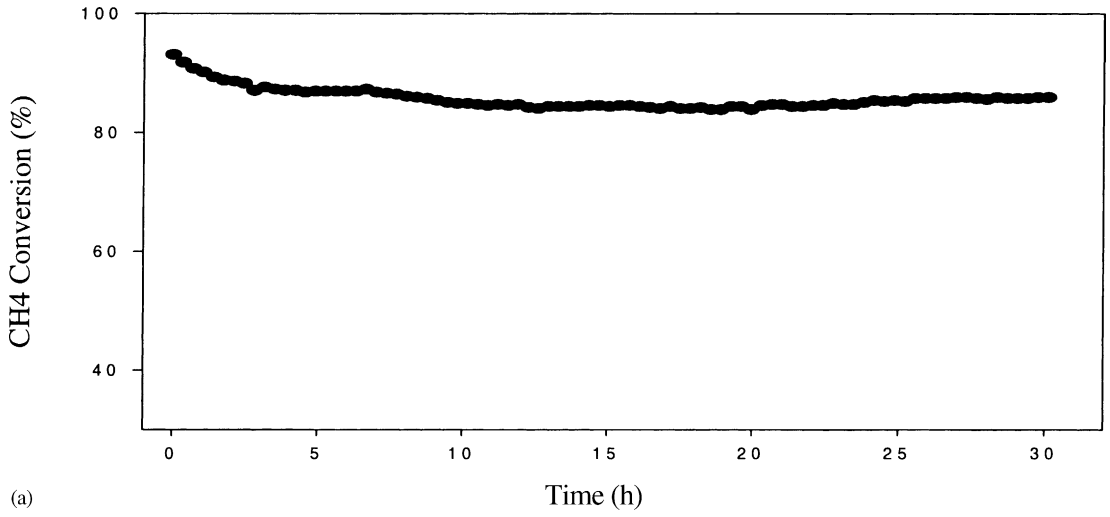

(a)

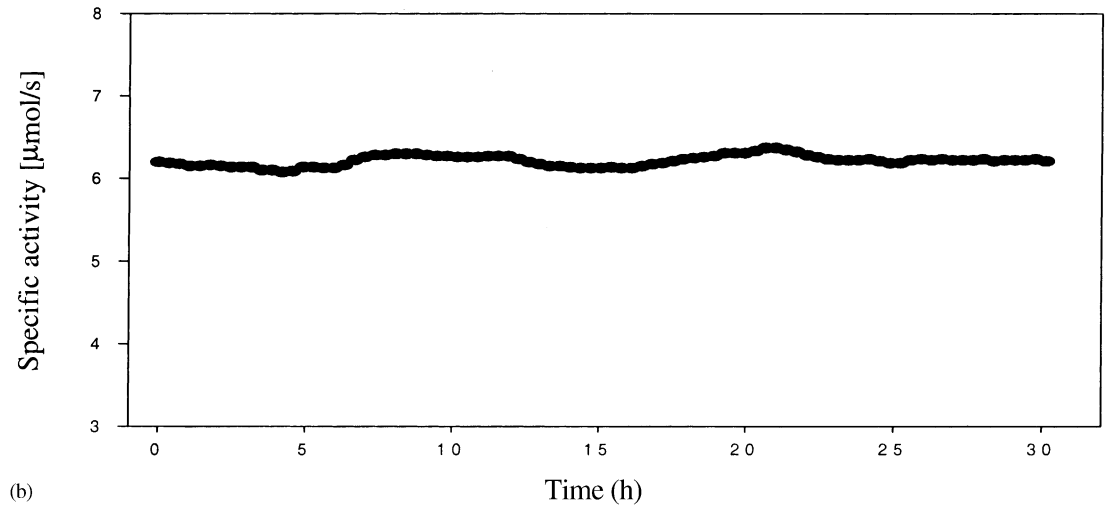

(b)

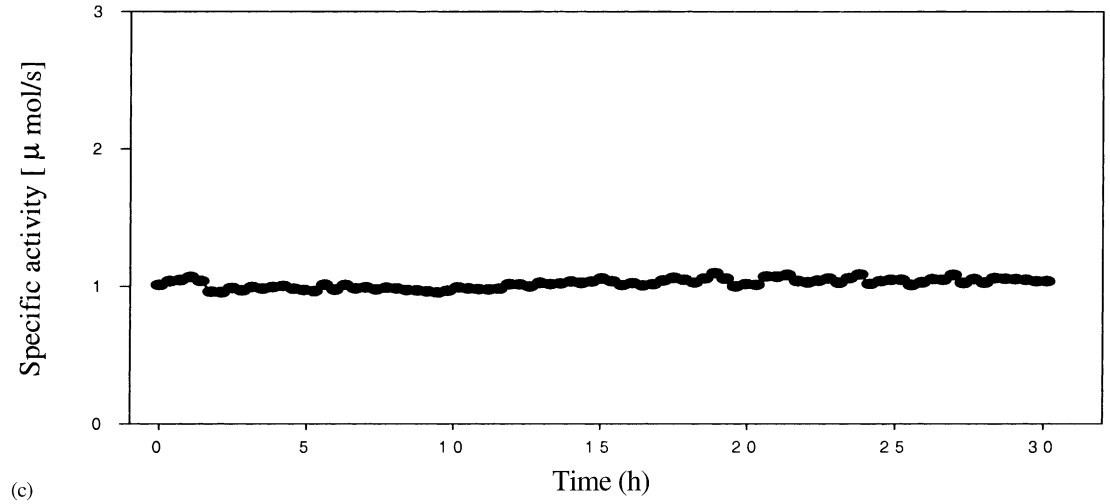

(c)

Fig. 8. (a) Methane conversion, and specific activities of (b) H_2 and (c) CO formation over Ni(60)SDC anode under open-circuit condition as function of time (operating conditions: same as in Fig. 1).

Table 2
Carbon formation based on TPO analyses of samples collected at top and bottom layers of Ni(30)SDC and Ni(60)SDC anodes after 30 h of operation[a]

	Top layer of anode		Bottom layer of anode	
	Carbon in sample (mg)	Carbon in sample (%)	Carbon in sample (mg)	Carbon in sample (%)
Ni(30)SDC	17.15	85.8	4.28	21.4
Ni(60)SDC	19.21	96.0	2.57	12.9

[a] Operating conditions of TPO: 50% O_2 in Ar; 1 atm; 10 °C min^{-1} from 25 to 900 °C; total flow rate: 30 ml min^{-1}; sample weight: 20 mg.

and then sampled for TPO tests. The results are listed in Table 2. Indeed, it is seen that the bottom layer of coke formed over the Ni(60)SDC anode is less than that over Ni(30)SDC. Note that, the bottom layer of coke will deactivate the anode but the top layer may not. This confirms this influence of the beneficial structure of Ni(60)SDC shown above. As a result, the Ni(60)SDC anode is deactivated less readily and thus displays improved activity and stability.

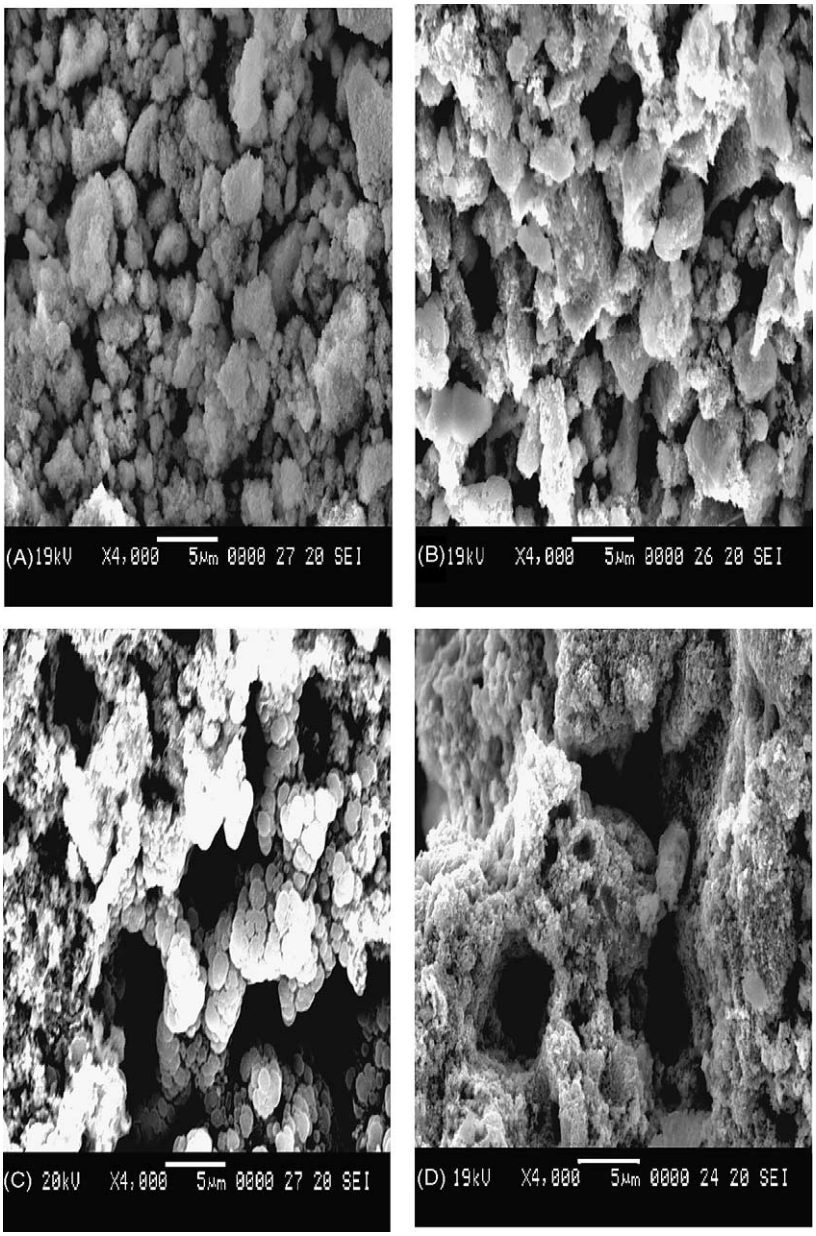

Fig. 9. Electron micrographs of Ni-SDC anodic structures with nickel content of: (A) 40 wt.%, (B) 50 wt.%, (C) 60 wt.%, and (D) 70 wt.%.

With a view to addressing further the effect of anodic microstructure on the polarization and performance of the Ni-SDC anodes, SEM studies were conducted for different nickel loadings. The morphologies of Ni-SDC anodes with 40 and 50 wt.% Ni (Fig. 9(A) and (B)) are composed of loosely-connected grains, i.e. well-packed and closely-connected Ni–Ni skeletons are not formed because of inadequate Ni loading. Consequently, substantially lower electron transfer rates and much fewer active sites would be encountered with these anodes to facilitate the occurrence of anodic polarization. When the Ni content is increased to 70 wt.%, however, the particles are well sintered (Fig. 9(D)). This results in a detrimental structure of SDC which is heavily covered or surrounded by nickel and is accompanied by a great loss of porosity. This, in turn, reduces the reaction area of the TPB, which leads to decreased efficiency of the anode and, hence, to its susceptibility of being polarized.

From the above findings and the morphology of the Ni-SDC anode with 60 wt.% Ni (Fig. 9(C)), it can be concluded that the distribution and connection between Ni–Ni, SDC–SDC and Ni-SDC particles were optimized with this anode and provided rich TPB sites for the anodic reaction; nickel particles form a skeleton with well-connected SDC grains finely distributed over the Ni grain surfaces [18]. In this regard, it is expected that at this nickel content the migration and coalescence of Ni particles are inhibited by the well-connected SDC network. The capacities of nickel particles as the main electrocatalytic sites, and of SDC particles serving as the supplier of O^{2-}, are optimized with the Ni(60)SDC anode. Accordingly, the Ni-SDC anode with 60 wt.% Ni exhibits the most desirable features among the anodes tested, namely: low polarization, high performance, and good stability. The results and discussion above clearly establish that the microstructure of the Ni-SDC anode has significant implications on the polarization, activity and stability of the electrode for direct oxidation of methane.

4. Conclusions

A Ni-SDC anode is evaluated for the direct electrochemical oxidation of methane in SOFCs with an YSZ electrolyte. The following conclusions can be drawn:

1. Ni-SDC anodes exhibit higher OCV and a lower degree of polarization compared with those of Ni-YSZ, presumably due to the fact that YSZ is a purely ionic conductor and SDC is capable of conducting both ions and electrons. In this aspect, Ni-SDC is a better anodic electrocatalyst for SOFCs.
2. A Ni-SDC anode with 60 wt.% Ni displays the highest values of OCV and limiting current. This is attributable to the optimized microstructure which provides the most electrochemical active sites at the TPB and leads to the least degree of anodic polarization.
3. The anodic polarization may results from the effect of concentration polarization, that is, the reaction rate in the close proximity of the anode surface is higher than the O^{2-} supply rate to the active sites at the TPB and the rate of release of lattice oxygen anions from SDC.
4. Under open-circuit conditions for 30 h, the Ni(60)SDC anode exhibits high catalytic activity and stability even though coking occurs to a certain extent. This is presumably due to the optimized distribution and connection between Ni–Ni, SDC–SDC and Ni-SDC particles in this anode. A closely-packed Ni skeleton is formed with the well-connected SDC grains finely distributed over the Ni grain surfaces. This inhibits the internal growth of carbonaceous deposits and, hence, prevents damage to the internal structure of the anode.

References

[1] J.N. Armor, Appl. Catal. A 176 (1999) 159.
[2] E.P. Murray, T. Tsai, S.A. Barnett, Nature 400 (1999) 649.
[3] R.J. Gorte, S. Park, J.M. Vohs, C. Wang, Adv. Mater. 12 (2000) 1465.
[4] H.C. Yao, Y.F. Yu Yao, J. Catal. 86 (1984) 254.
[5] J.C. Summers, S.A. Ausen, J. Catal. 58 (1979) 131.
[6] Q. Zhang, Y. Qin, L. Chang, Appl. Catal. 70 (1991) 1.
[7] V.D. Belyaev, T.I. Politova, O.A. Marina, V.A. Sobyanin, Appl. Catal. A 133 (1995) 47.
[8] O.A. Marina, M. Mogensen, Appl. Catal. A 189 (1999) 117.
[9] R.J. Gorte, H. Kim, J.M. Vohs, J. Power Sources 106 (2002) 10.
[10] B.C.H. Steele, I. Kelly, P.H. Middleton, R. Rudkin, Solid State Ionics 28 (1988) 1547.
[11] B.C.H. Steele, P.H. Middleton, R. Rudkin, Solid State Ionics 40 (1990) 388.
[12] E.S. Putna, J. Stubenrauch, J.M. Vohs, R.J. Gorte, Langmuir 11 (1995) 4832.
[13] K. Eguchi, T. Setoguchi, T. Inoue, M. Arai, Solid State Ionics 52 (1992) 165.
[14] H. Uchida, H. Suzuki, M. Watanabe, J. Electrochem. Soc. 145 (1998) 615.
[15] T.H. Etsell, S.N. Flengas, Chem. Rev. 70 (1970) 339.
[16] H. Yahiro, Y. Eguchi, K. Eguchi, H. Arai, J. Appl. Electrochem. 18 (1988) 527.
[17] R. Maric, S. Ohara, T. Fukui, T. Inagaki, J.I. Fujita, Electrochem. Solid-State Lett. 1 (1998) 201.
[18] X. Zhang, S. Ohara, R. Maric, K. Mukai, T. Fukui, H. Yoshida, M. Nishimura, T. Inagaki, K. Miura, J. Power Sources 83 (1999) 170.
[19] S. Ohara, R. Maric, X. Zhang, K. Mukai, T. Fukui, H. Yoshida, T. Inagaki, K. Miura, J. Power Sources 86 (2000) 455.